Proceedings of the 19th World Congress
The International Federation of Automatic Control
Cape Town, South Africa. August 24-29, 2014

Distributed Thermal-Electrochemical Modeling of a Lithium-Ion Battery to Study the Effect of High Charging Rates

Sohel Anwar*, Changfu Zou, Chris Manzie****

**Department of Mechanical Engineering, Purdue School of Engineering and Technology, IUPUI, Indianapolis, USA (e-mail: soanwar@iupui.edu)*
***Department of Mechanical Engineering, University of Melbourne, VIC 3010, Australia (email: changfu.zou@unimelb.edu.au, manziec@unimelb.edu.au)*

Abstract: In this paper, we investigate distributed thermal-electrochemical modeling of a Lithium-Ion battery cell to include the effect of temperature distribution across the thickness of the cell as a first step to study the module level temperature distribution at high charging rates. Most recent works have focused on lumped thermal models for a Li-Ion cell which ignore any temperature differential across cell thickness. However, even a small temperature differential across cell thickness at the cell level can contribute to significant temperature differential in the thickness direction of stacked-up Li-Ion cells at the module level. Such temperature differential can potentially impact the battery charging control system, especially at high charging rates. Here, the thermal-electrochemical partial differential and algebraic equations for a Li-ion cell are solved via a spatial finite difference method. Simulation results show that the temperature differentials over the cell thickness at the cell level are not insignificant, particularly at high charging rates.

1. INTRODUCTION

Lithium-Ion batteries are a major focus for developing advanced energy storage systems, particularly for use in the transportation sector. These batteries possess a number of characteristics that make them well suited for automotive applications, namely high energy density, high discharge power, low memory effect resulting into good cycle performance and battery life. Further advancements in these performance characteristics are limited by electrochemical as well as thermal capabilities of a lithium ion battery module. Recent events of battery failures due to thermal runaway with $LiCoO_2$ chemistry in aircraft applications further confirm the challenges that lied ahead. Such challenges cannot be fully addressed without a comprehensive understanding of the battery's electrochemical and thermal behavior under a wide range of operating conditions.

The majority of the work related to the thermal modeling of Lithium-Ion batteries previously focused on lump parameter models. While this assumption of uniform temperature distribution across cell thickness is reasonable for a single cell, the same is less likely to hold good for a module where a number of cells are stacked together. Wang et al. (1998) presented a micro-macroscopic coupled model for batteries and fuel cells. No thermal model for the battery was presented in this work. Chaturvedi et al. (2010) discussed electrochemical model based algorithms for Li-Ion battery management systems while Klein et al. (2013) presented an electrochemical model based observer design that included lumped thermal model for a Li-Ion cell. Rao and Newman (1997) developed a general energy balance equation for insertion battery system that captures heat generation mechanisms. This model is based on lumped parameters with average temperature of the cell as the state variable. Gu and Wang (2000) presented a distributed thermal model with associated heat generation mechanism in a Li-Ion cell. However, the model was then simplified to lumped parameter model which ignored any temperature differential across the cell thickness. The average cell temperature was then used in an Arrhenius type equation to update the electrochemical model parameters. Thomas et al. (2002) analyzes the Bernardi's thermal model for Lithium Ion cells developed via a general energy balance for electrochemical systems. However, this is a lumped parameter model with respect to cell temperature. It also uses volume averaged parameters and aggregate of state variables to determine average cell temperature. Chen et al (2005) presented a distributed thermal model and analysis between ten different approximations the original 3D model in order to estimate the accuracy of those models. However, they used experimental data to obtain necessary information for computing the heat generation rate. Kumaresan et al (2008) used a lumped parameter thermal model of a Li-Ion cell to predict the discharge performance at different operating temperatures. They compared the simulation results with experimental data for Li-Ion pouch cell (prismatic). Cai and White (2011) used COMSOL to study the thermal effects on the cell behavior during galvanostatic discharge process with and without a pulse. Although the open circuit potential of the cell and a few other parameters were updated as a function of temperature change, thermal behavior of the cell during charging was not studied. Khateeb et al (2004) provides an innovative design of phase change material thermal management system of a Li-Ion battery for electric scooter

application that did not use any cooling fan. Their analysis used nine $LiFePO_4$ based cell for the module with only natural convection which was claim to provide sufficient cooling of the battery for such applications.

As indicated earlier, a comprehensive understanding of Li-Ion battery thermal behavior can potentially offer efficient ways to design battery management systems via optimization of charging and discharging control algorithms. In this paper, we combine the distributed thermal model of a Li-Ion cell with the electrochemical model to obtain the heat generation rate and then investigate the effect of temperature distribution in a Li-Ion cell. Investigation of the temperature differential in the thickness direction at module level is currently underway which builds on the findings of the current work.

2. MODELING OF LITHIUM-ION CELL

A majority of electro-chemistry based Li-Ion battery models utilize simultaneous computation of concentration and potential fields of electrode active materials and electrolyte. Doyle et al (1993) presented a model for a lithium ion cell that consists of porous electrodes and a separator. This model was based on concentrated solution theory (1975). Many other Li-Ion battery models were presented based on Doyle's work that included additional aspects of concentrated solution theory and porous electrode theory, and had good performance in capturing battery electrochemical kinetics (Fuller et al., 1994a, 1994b), (Doyle et al., 1996), (Thomas & Newman, 2003), (Arora, et al., 2000), (Ramadass et al., 2003, 2004), (Ning et al., 2006), (Botte et al., 2000), (Gomadam et al., 2002), (Santhanagopalan et al., 2006). Circuit based or empirical Li-Ion models have been well studied in the literature, but they do not capture the electro-chemical kinetics at various operating conditions. Hence we have adopted an electro-chemistry based Li-Ion model for improved accuracy. Volume-averaging along with polynomial approximation for the solid phase concentration dynamics has worked well, especially for the temperature distribution within a cell (Balakotaiah & Chakraborty, 2003)-(Chang & Balakotaiah, 2003). The electrochemical model of a Li-Ion cell presented in (Chaturvedi et al., 2010) and (Klein et al., 2013) follow a similar method and is leveraged in our distributed model development. The following sets of partial differential equations represent such a model.

$$\varepsilon_e \frac{\partial c_e(x,t)}{\partial t} = \frac{\partial}{\partial x}\left[D_e \frac{\partial c_e(x,t)}{\partial x} + \frac{1-t_c^0}{F} i_e(x,t)\right]$$

$$\frac{\partial \phi_e(x,t)}{\partial x} = -\frac{i_e(x,t)}{\kappa} + \frac{2RT(x,t)}{F}[1-t_c^0] * \left[1 + \frac{d(\ln f_{c/a})}{d(\ln c_e(x,t))}\right]\frac{\partial \ln c_e(x,t)}{\partial x}$$

$$\frac{\partial c_{s,j}(x,r,t)}{\partial t} = \frac{1}{r^2}\frac{\partial}{\partial r}\left[D_{s,j} r^2 \frac{\partial c_{s,j}(x,r,t)}{\partial r}\right]$$

$$\frac{\partial \phi_s(x,t)}{\partial x} = \left[\frac{i_e(x,t) \pm I(t)}{\sigma}\right]$$

$$\frac{\partial i_e(x,t)}{\partial x} = \sum_{j=1}^{n} \frac{3\varepsilon_{s,j}}{R_{p,j}} F j_{n,j}(x,t) \qquad (1)$$

$$j_{n,j}(x,t) = \frac{i_{0,j}(x,t)}{F}\left[e^{\alpha_a F \eta_j(x,t)/RT(x,t)} - e^{-\alpha_c F \eta_j(x,t)/RT(x,t)}\right]$$

$$i_{0,j}(x,t) = r_{eff,j} c_{e,j}(x,t)^{\alpha_a}\left[c_{s,j}^{max} - c_{ss,j}(x,t)\right]^{\alpha_a} c_{ss,j}(x,t)^{\alpha_c}$$

$$\eta_j(x,t) = \phi_s(x,t) - \phi_e(x,t) - U\left(c_{ss,j}(x,t)\right) - FR_{f,j}(x,t) j_{n,j}(x,t)$$

where D_e, $D_{s,j}$ are effective Diffusion coefficients of electrolyte and solid phase, c_e, $c_{s,j}$, $c_{ss,j}$ are Lithium concentration in electrolyte, active material of electrodes, and surface of solid particles, ε_e, $\varepsilon_{s,j}$ are volume fractions of electrolyte and solid phase, r, x are radius of particle, thickness direction variable, T, R, F are temperature, universal gas constant, Faraday's constant, ϕ_e, ϕ_s are potential in the electrolyte and in the solid phase, i_e, $i_{0,j}$ are ionic current in electrolyte and exchange current, t^o_c, $f_{c/a}$, α_a, α_c are model parameters, η_j is the over potential for main reaction, $j_{n,j}$ is the molar fluxes between active electrode material and electrolyte, σ, κ are ionic conductivities of the electrode and electrolyte, U, I are Open circuit potential between of active electrode material, Current flow through separator. The thermal model that can be integrated with the above electrochemical model equations is given by (Gu & Wang, 2000) the following equations:

$$\rho_k c_{pk}\left(\frac{\partial T_k}{\partial t} + \underline{v_k}.\underline{\nabla} T_k\right) = -\underline{\nabla}.\underline{q_k} + \sum_{species} \widehat{H_k}\underline{\nabla}.\underline{J_k} \qquad (2)$$

where λ, h, c_p are thermal conductivity, surface heat transfer coefficient, specific heat at constant pressure, k represents the phases (e.g. solid, electrolyte). Now the convection term (2nd term on left side of the above equation) is generally small due to the fact that the species velocities are very small and that the cell is very thin further limiting the species velocities. As a result this term can be neglected (Gu & Wang, 2000). Thus the above thermal model can be reduced to the following equation:

$$\rho_k c_{pk}\left(\frac{\partial T_k}{\partial t}\right) = -\underline{\nabla}.\underline{q_k} + \sum_{species} \widehat{H_k}\underline{\nabla}.\underline{J_k} \qquad (3)$$

The right side of the above equation represents heat generation and conduction which can be rewritten as (Gu & Wang, 2000):

$$\rho_k c_{pk}\left(\frac{\partial T_k}{\partial t}\right) = \underline{\nabla}.\left(\lambda_k \underline{\nabla} T_k\right) - \underline{i_k}.\underline{\nabla}\phi_k$$

The first term on right side of the above equation accounts for heat conduction while the second term represents the heat generation. Using representative elemental volume (REV) for each species, the above thermal model can be re-written as follows:

$$\left(\frac{\partial(\rho c_p T)}{\partial t}\right) = \underline{\nabla}.\left(\lambda \underline{\nabla} T\right) + q$$

$$\rho c_p = \sum_k \varepsilon_k \rho_k c_{pk} \qquad \lambda = \sum_k (\lambda_k^{eff} + \lambda_{a,k}) \qquad (4)$$

$$q = -\sum_j a_{sj} i_{nj}\left(U_j - T\frac{\partial U_j}{\partial T}\right) + \sum_j a_{sj} i_{nj}(\phi_{se} - \phi_{es}) + \sum_{k\neq m}\sum_m (\Delta h^* \Gamma_{km}) - \sum_{k=e\&s}\left(< \underline{i_k} >.\nabla < \phi_k >\right) \qquad (5)$$

Where, $\Delta h^* = (h_k - h_m) + (c_{pk} - c_{pm})T$.

2.1 Integration of Thermal Effects into Electrochemical Model for Lithium Ion Battery

According to the most prevalent literature, a number of Li-Ion battery model parameters are subject to significant variations with respect to varying temperature within the cell (Klein et al, 2013). In particular, the ionic conductivity in the electrolyte and the electrolyte diffusion coefficients are strong functions of temperature for LIB. One possible way to include thermal effect into the electrochemical model is to use an Arrhenius type equation:

$$p = p_{ref}\, e^{\left[\frac{E_{act,p}}{R}\left(\frac{1}{T_{ref}} - \frac{1}{T}\right)\right]} \tag{6}$$

The temperature distribution can be averaged over the volume of LIB cell in order to use the lumped Arrhenius equation for parameter update. The block diagram in Fig. 1 can be used to integrate the thermal aspects into the electrochemical equations.

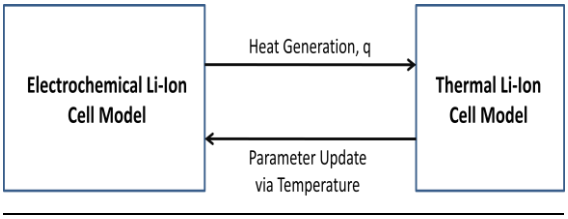

Figure 1: Electrochemical model parameter update base on temperature via Arrhenius equation.

2.2 Model Reduction to 1-D Case

A reasonable assumption is that the temperature differential is present only in the thickness direction of the cell. While some papers assume the absence of such a differential for a cell, it would be less accurate for a Li-Ion module where the cells are stacked against each other. Even a small temperature differential across the thickness of the cell may result into appreciable temperature differential across the module. Keeping this in mind we reduce the thermal model to only x direction which is the direction of cell thickness. The electrochemical model presented previously is already a 1-D model.

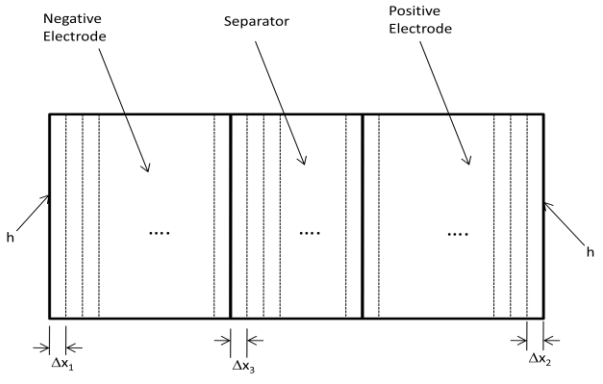

Figure 2: 1-D spatial discretization of Li-Ion cell.

1-D Thermal Model:

$$\left(\frac{\partial(\rho c_p T)}{\partial t}\right) = \frac{\partial}{\partial x}\left(\lambda \frac{\partial T}{\partial x}\right) + q \tag{7}$$

We would like to utilize finite difference method in the spatial domain by discretization which will render the above PDE to a set of ODE's. Each of the electrodes and the separator are discretized spatially in a finite number of elements. Assuming that the spatial domain (x) is discretized in N number of elements and that the thermal conductivity is constant over the discrete element, we obtain the following set of ODE's:

$$\left(\frac{d(\rho_i c_{pi} T_i)}{dt}\right) = \lambda_i \frac{T_{i+1} - 2T_i + T_{i-1}}{(\Delta x)^2} + q_i \quad where\ i = 1,2, \dots N \tag{8}$$

The initial and boundary conditions are given by:

$$T_1(t)|_{t=0} = T_2(t)|_{t=0} = \cdots = T_N(t)|_{t=0} = T_{amb}$$

$$\left(\frac{d(\rho_1 c_{p1} T_1)}{dt}\right) = \lambda_1 \frac{T_2 - 2T_1 + T_0}{(\Delta x)^2} + q_1 - \frac{h(T_1 - T_{amb})}{\Delta x} \tag{9}$$

$$\left(\frac{d(\rho_N c_{pN} T_N)}{dt}\right) = \lambda_N \frac{T_{N+1} - 2T_N + T_{N-1}}{(\Delta x)^2} + q_N - \frac{h(T_N - T_{amb})}{\Delta x}$$

The thermal properties of each element are computed based on its location (either in positive or negative electrode or separator) using volume averaging of component properties (e.g. $LiCoO_2$, Liquid electrolyte, Graphite, Separator material).

Now the heat generation term is given by:

$$q_i = -\frac{1}{V_i}\int_{V_i} \sum_j a_{sj} i_{nj} \left(U_j - T\frac{\partial U_j}{\partial T}\right) dv + \frac{1}{V_i}\int_{V_i} \sum_j a_{sj} i_{nj} (\phi_{se} - \phi_{es})\, dv + \frac{1}{V_i}\int_{V_i} \sum_{k \neq m} \sum_m (\Delta h^* \Gamma_{km})\, dv - \frac{1}{V_i}\int_{V_i} \sum_{k=e\&s} \left(< \underline{i_k} >. \nabla < \phi_k >\right) dv \tag{10}$$

Where V_i is the volume of each element. Assuming that the heat effect due to the electrical non-equilibrium is negligible (Gu & Wang, 2000), we obtain:

$$\frac{1}{V_i}\int_{V_i} \sum_j a_{sj} i_{nj} (\phi_{se} - \phi_{es})\, dv = \frac{1}{V_i}\int_{V_i} \sum_j a_{sj} i_{nj} (< \phi_s > - < \phi_e >)\, dv \tag{11}$$

Furthermore conservation of charge in both solid and electrolyte phases requires that (Wang et al., 1998):

$$\nabla. < i_e > = -\nabla. < i_s > = \sum_j a_{sj} i_{nj} \tag{12}$$

Then the above term can be integrated by parts and can be rewritten as:

$$-\frac{1}{V_i}\int_{V_i} \nabla. < i_e > < \phi_{e>} dv - \frac{1}{V_i}\int_{V_i} \nabla. < i_s > < \phi_{s>} dv = -\sum_{k=e\&s} < i_k > < \phi_{k>} + \frac{1}{V_i}\int_{V_i} \sum_{k=e\&s} < i_k >. \nabla < \phi_{k>}\, dv = -I * V_{el}^i + \frac{1}{V_i}\int_{V_i} \sum_{k=e\&s} < i_k >. \nabla < \phi_{k>}\, dv \tag{13}$$

where V^i_{el} is the voltage drop across an element. The heat generation term is then given by,

$$q_i = -\frac{1}{V_i}\int_{V_i}\sum_j a_{sj} i_{nj}\left(U_j - T\frac{\partial U_j}{\partial T}\right)dv - I * V_{el}^i + \frac{1}{V_i}\int_{V_i}\sum_{k\neq m}\sum_m(\Delta h^* \Gamma_{km})\,dv \quad (14)$$

As a simplifying approximation, we assume that the phase transformation term is small and hence this term is omitted. Thus the heat generation term can be written as:

$$q_i = -\frac{1}{V_i}\int_{V_i}\sum_j a_{sj} i_{nj}\left(U_j - T\frac{\partial U_j}{\partial T}\right)dv - I * V_{el}^i \quad (15)$$

The localized reactions for Li-Ion battery are:

Anode:
$Li \leftrightarrow Li^+ + e^-$
Cathode:
$Li^+ + e^- + \theta_s \leftrightarrow Li + \theta_s$ (16)

Since there is only one pair of reaction, two further simplifying assumptions are made: i) the OCP U_j is same for the both reactions; and ii) the electrode reaction rates are spatially uniform. The heat generation equation can then be rewritten as:

$$q_i = -\sum_j I_j\left(U_j^i - T\frac{\partial U_j^i}{\partial T}\right) - I * V_{el}^i \quad (17)$$

Where, $I_j = \frac{1}{V_i}\int_{V_i} a_{sj} i_{nj} dv$ and U_j^i is the OCP for element i for j-th reaction.

Equations (1) and (8) in the previous section represent the distributed thermal – electrochemical model. Additionally, continuity of solution requires that:

$$T_{\mathrm{N}+1}^{neg} = T_1^{sep}$$
$$T_{\mathrm{N}+1}^{pos} = T_{\mathrm{N}+1}^{sep}$$
$$\lambda_{neg}\frac{T_{N+1}^{neg} - T_N^{neg}}{\Delta x_{\mathrm{neg}}} = \lambda_{sep}\frac{T_2^{sep} - T_1^{sep}}{\Delta x_{\mathrm{sep}}} \quad (18)$$
$$\lambda_{sep}\frac{T_{N+1}^{sep} - T_N^{sep}}{\Delta x_{\mathrm{sep}}} = -\lambda_{pos}\frac{T_{N+1}^{pos} - T_N^{pos}}{\Delta x_{\mathrm{pos}}}$$
$$U_j^i = Open\ circuit\ or\ equivalent\ portential\ of\ reaction\ j$$

$$q_i = -\sum_j I_j\left(U_j^i - T\frac{\partial U_j^i}{\partial T}\right) - I * V_{el}^i$$

$$I_j = \frac{1}{V_i}\int_{V_i} a_{sj} i_{nj} dv \quad (19)$$

Since V_i is elemental volume and the transfer current density is assumed to be uniform over the area perpendicular to the thickness direction, I_j can be simplified as follows:

$$I_j = \frac{1}{V_i}\int_{V_i} a_{sj} i_{nj} dv = \frac{1}{\Delta x}\int_0^{\Delta x} a_{sj} i_{nj} dx \quad (20)$$

When Δx is sufficiently small, the above relationship can be rewritten as:

$$I_j = \frac{1}{\Delta x}\int_0^{\Delta x} a_{sj} i_{nj} dx \approx a_{sj} i_{nj} \quad (21)$$

Also, we note that:

$$\nabla.< i_e >= -\nabla.< i_s >= \sum_j a_{sj} i_{nj} \quad (22)$$

$$\frac{\partial i_e(x,t)}{\partial x} = \sum_{j=1}^{n}\frac{3\varepsilon_{s,j}}{R_{p,j}} F j_{n,j}(x,t)$$

Comparing these two equations, we can write:

$$a_{sj} i_{nj} = \frac{3\varepsilon_{s,j}}{R_{p,j}} F j_{n,j}(x,t) \quad (23)$$

Additionally, $i_s + i_e = I$. V_{el}^i can be computed as using the original relationship as follows:

$$I * V_{el}^i = \sum_{k=e\&s} < i_k >< \phi_k > \quad (24)$$

Both i_k and ϕ_k are computed from the electrochemical model.

As indicated earlier, the heat capacity of each element is computed via volume averaging based on location (e.g. anode, cathode, and separator). However, the thermal conductivity of each element is computed based on the assumption that the materials (e.g. active material and electrolyte) are collocated so that their equivalent thermal conduction properties can be that of a layered structure (7). The following equivalent thermal conductivity equation is used for positive and negative electrodes.

$$\lambda_i = \frac{\sum_k \varepsilon_k}{\sum_k \varepsilon_k/\lambda_k}$$

Since the separator is mostly filled with the liquid electrolyte, thermal conductivity of the electrolyte is used for locations in the separator region.

3. Simulation Results

The simplified Li-Ion cell model in section 2 was simulated using OpenModelica platform. We focused on charge / overcharge input to the model. The cell chemistry was chosen to simulate a Li-Ion cell with $LiCoO_2$ cathode with a capacity of 6Ah. Three different charging rates were applied, namely 1C, 5C, and 10C rates. The cell thermal and electrochemical parameters were obtained from (Smith & Wang, 2006) and are shown in Tables 1 and 2, respectively. Additional data can also be found in (Subramanian et al., 2009)-(Zhang et al, 2014).

The average surface heat transfer coefficient at cell boundaries for natural convection in a Li-Ion cell is reported to be in the range of 2-10 W/m^2/K (Chen et al, 2005). For the current work, the average heat transfer coefficient at the cell boundaries has been assumed to be 5 W/m^2/K. The number of elements in the spatial discretization for each of the zones (i.e. negative & positive electrodes, and separator) is assumed to be N = 5. The following values are assumed for R and F: R = 8.31, F = 96485.

The temperature for each of the elements was simulated in time. When the temperature of the element stabilized to a steady state value for a particular charge rate, this temperature was recorded for all elements. A spatial plot of this steady state temperature was performed to visualize any temperature differential across the electrodes and the separator.

Table 1: Thermal parameters of Li-Ion cell ($LiCoO_2$).

Parameter	Neg.Electrode	Separator	Pos.Electrode
λ, W/m/K	0.824	0.38	0.92
ρ, kg/m^3	1269.73	1042.4	1796.34
c_p, J/kg/m	1657.92	1999.4	1618.2
Thickness, m	0.000116	0.000035	0.00014
dU/dT, V/K	0.00022		0.00022
ε solid	0.643		0.556
ε		0.276	
ε electrolyte	0.357	0.724	0.444

Table 2: Electrochemical parameters of the Li-Ion cell.

Parameter	Neg. Electrode	Separator	Pos. Electrode
Ds	3.9E-14		1.0E-13
De	1.6E-11	7.5E-11	2.2E-11
t^0_c		0.363	
R_p	0.0000125		0.000008
σ	32.3		0.6151

The temperature distributions, thus obtained, were then plotted in the thickness direction of the cell and are shown in Figures 3 through 5 for each of the charge rates. Figure 3 shows the temperature differential across the cell for 1C charge rate.

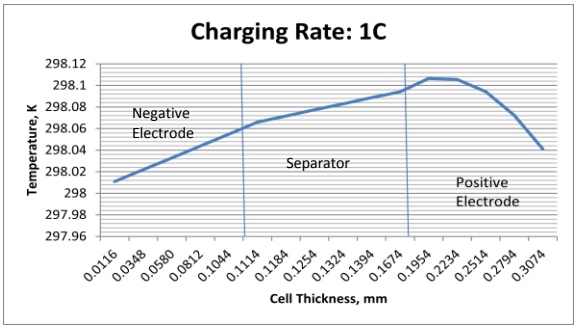

Figure 3: Temperature distribution at 1C charging rate.

The variation in the temperature across cell thickness is very small and can be ignored for most practical purposes. However, when the charging rate reaches 5C, an appreciable temperature differential is observed (Fig. 4). Although the range of the temperature variation is within 3 degree Celsius, this scale of temperature could easily be amplified when cells are stacked up in a module.

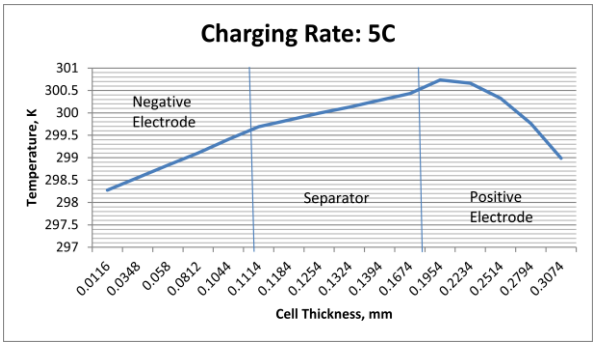

Figure 4: Temperature distribution at 5C charging rate.

For a very fast charging scenario, a 10C charge rate is applied to the cell. The resulting temperature variation is shown in figure 5 which shows significant temperature differential along cell thickness. The range of temperature variation is about 11 degree Celsius which has the potential of causing significant deterioration at the module level if not actively controlled by the battery management system. The sizable temperature rise for 10C charging rates is tied to the compounding factors of heat generation within the cell and limited heat transfer to the ambient.

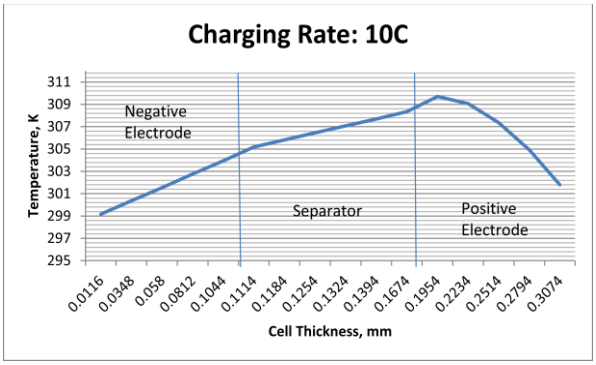

Figure 5: Temperature distribution at 10C charging rate.

4. Conclusion

We developed a distributed thermal model of Li-Ion cell with $LiCoO_2$ cathode based on electro-chemical equations in order to study the temperature differential across cell thickness of a Li-Ion cell. The distributed model was discretized in spatial domain and solved for temperature distribution across cell thickness for various charging rates. Simulation results show that although the temperature differential was not significant at low charging rates, there was appreciable differential of temperature across cell thickness for rapid charge situations such as 5C or 10C rates. These temperature differentials are likely to grow larger when the cells are stacked up in a module due to variations in thermal conductivity and heat transfer coefficients at the cell interfaces. Such a study is currently under way that involves module level distributed thermal-electrochemical modeling of a Li-Ion cell.

References

Wang, C.Y., W.B. Gu, and B.Y. Liaw (1998). Micro-Macroscopic Coupled Modeling of Batteries and Fuel Cells: I. Model Development. *Journal of Electrochemical Society*, 145, (10), 3407-3417.

Chaturvedi, N.A., R. Klein, J. Christensen, J. Ahmed, and A. Kojic (2010). Algorithms for Advanced Battery-Management Systems: Modeling, Estimation, and Control Challenges for Lithium-Ion Batteries. *IEEE Control Systems Magazine*, June, 49-68.

Klein, R., N.A. Chaturvedi, J. Christensen, J. Ahmed, R. Findeisen, and A. Kojic (2013). Electrochemical Model Based Observer Design fo a Lithium-Ion Battery. *IEEE*

Transactions on Control Systems Technology, 21, n(2), 289-301.

Rao, L. and J. Newman (1997). Heat-Generation Rate and General Energy Balance for Insertion Battery System. *Journal of the Electrochemical Society*, 144, (8), 2697-2704.

Gu, W.B. and C.Y. Wang (2000). Thermal-Electrochemical Modeling of Battery Systems. *Journal of the Electrochemical Society*, 147, (8), 2910-2922.

Thomas, K.E., J. Newman, and R.M. Darling (2002). Mathematical Modeling of Lithium Batteries. *Chapter in book titled 'Advanced in Lithium-Ion Batteries'*, edited by W. van Schalkwijk and B. Scrosati, Kluwer Academic/Plenum Publisher.

Chen, S.S., C.C. Wan, and Y.Y. Wang (2005). Thermal Analysis of Lithium-Ion Batteries. *Journal of Power Sources*, 140, 111-124.

Kumaresan, K., G. Sikha, and R.E. White (2008). Thermal Model for a Li-Ion Cell. *Journal of the Electrochemical Society*, 155, (2), A164-A171.

Cai, L. and R.E. White (2011). Mathematical Modleing of Lithium Ion Battery with Thermal Effects in COMSOL Inc. Multiphysics Software. *Journal of Power Sources*, 196, 5985-5989.

Khateeb, S.A., M.M. Farid, J.R. Selman, and S. Al-Hallaj (2004). Design and Simulation of a Lithium-Ion Battery with Phase Change Material Thermal Management System for an Electric Scooter. *Journal of Power Sources*, 128, 292-307.

Doyle, M., T.F. Fuller, and J. Newman (1993). Modeling of Galvanostatic Charge and Discharge of the Lithium/Polymer/Insertion Cell. *Journal of Electrochemical Society*, 140, 1526-1533.

Newman, J. and W. Tiedermann (1975). Porous-electrode theory with battery applications. *AIChE Journal*, 21, 25-41.

Fuller, T.F., M. Doyle, and J. Newman (1994). Simulation and Optimization of the Dual Lithium Ion Insertion Cell. *Journal of Electrochemical Society*, 141, 1-10.

Fuller, T.F., M. Doyle, and J. Newman (1994). Relaxation Phenomena in Lithium-Ion-Insertion Cells. *Journal of Electrochemical Society*, 141, 982-990.

Doyle, M., J. Newman, A.S. Gozdz, C.N. Schmutz, and J.M. Tarascon (1996). Comparison of Modeling Predictions with Experimental Data from Plastic Lithium Ion Cells. *Journal of Electrochemical Society*, 143, 1890-1903.

Thomas, K.E. and J. Newman (2003). Thermal Modeling of Porous Insertion Electrodes. *Journal of Electrochemical Society*, 150, A176-A192.

Arora, P., M. Doyle, A.S. Gozdz, R.E. White, and J. Newman (2000). Comparison between computer simulations and experimental data for high-rate discharges of plastic lithium-ion batteries. *Journal of Power Sources*, 88, 219-231.

Ramadass, P., B. Haran, R.E. White, and B.N. Popov (2003). Mathematical modeling of the capacity fade of Li-ion cells. *Journal of Power Sources*, 123, 230-240.

Ramadass, P., B. Haran, P.M. Gomadam, R.E. White, and B.N. Popov (2004). Development of First Principles Capacity Fade Model for Li-Ion Cells. *Journal of Electrochemical Society*, 151, A196-A203.

Ning, G., R.E. White, and B.N. Popov (2006). A generalized cycle life model of rechargeable Li-ion batteries. *Electrochimica Acta*, 51, 2012-2022.

Botte, G.G., V.R. Subramanian, and R.E. White (2000). Mathematical modeling of secondary lithium batteries. *Electrochimica Acta*, 45, 2595-2609.

Gomadam, P.M., J.W. Weidner, R.A. Dougal, and R.E. White (2002). Mathematical modeling of lithium-ion and nickel battery systems. *Journal of Power Sources*, 110, 267-284.

Santhanagopalan, S., Q. Guo, P. Ramadass, and R.E. White (2006). Review of models for predicting the cycling performance of lithium ion batteries. *Journal of Power Sources*, 156, 620-628.

Balakotaiah, V. and S. Chakraborty (2003). Averaging theory and low-dimensional models for chemical reactors and reacting flows. *Chemical Engineering Science*, 58, 4769-4786.

Chang, H.-C. and V. Balakotaiah (2003). Hyperbolic Homogenized Models for Thermal and Solutal Dispersion. *SIAM Journal of Applied Mathematics*, 63, 1231-1258.

Smith, K. and C-Y. Wang (2006). Power and Thermal Characterization of a Lithium-Ion Battery Pack for Hybrid-Electric Vehicles. *Journal of Power Sources*, 160, 662-673.

Subramanian, V.R., V. Boovaragavan, V. Ramadesigan, and M. Arabandi (2009). Mathematical Model Reformulation for Lithium-Ion Battery Simulations: Galvanostatic Boundary Conditions. *Journal of the Electrochemical Society*, 156, (4), A260 - A271.

Zhang, Z., T. Zeng, Y. Lai, M. Jia, and J. Li (2014). A comparative study of different binders and their effects on electrochemical properties of $LiMn_2O_4$ cathode in lithium ion batteries. *Journal of Power Sources*, 247, 1-8.